Article

Current Biology

Phase-Locked Stimulation during Cortical Beta Oscillations Produces Bidirectional Synaptic Plasticity in Awake Monkeys

Highlights

- Stimulation triggered from cortical beta oscillations induces synaptic plasticity
- Synaptic potentiation or depression depends on oscillatory stimulation phase
- Plasticity effects last for up to a few seconds
- Effects are explained by spike-timing-dependent plasticity mechanisms

Authors

Stavros Zanos, Irene Rembado, Daofen Chen, Eberhard E. Fetz

Correspondence

stavroszanos@gmail.com (S.Z.), irene.rembado@gmail.com (I.R.), dc342b@nih.gov (D.C.), fetz@uw.edu (E.E.F.)

In Brief

Zanos et al. demonstrate that closed-loop, phase-locked cortical stimulation from beta oscillations in the sensorimotor cortex of monkeys induces short-term, bidirectional synaptic plasticity. This effect may explain the role of oscillations in attention, learning, and cortical reorganization.

Zanos et al., 2018, Current Biology *28*, 2515–2526
August 20, 2018
https://doi.org/10.1016/j.cub.2018.07.009

CellPress

Current Biology
Article

Phase-Locked Stimulation during Cortical Beta Oscillations Produces Bidirectional Synaptic Plasticity in Awake Monkeys

Stavros Zanos,[1,2,4,*] Irene Rembado,[2,*] Daofen Chen,[3,*] and Eberhard E. Fetz[2,*]
[1]Center for Bioelectronic Medicine, Feinstein Institute for Medical Research, 350 Community Drive, Manhasset NY 11030, USA
[2]Department of Physiology & Biophysics, University of Washington, 1705 NE Pacific St, Seattle, WA 98195, USA
[3]Division of Neuroscience, National Institutes of Neurological Disorders and Stroke, National Institutes of Health, 6001 Executive Boulevard, Bethesda, MD 20892, USA
[4]Lead Contact
*Correspondence: stavroszanos@gmail.com (S.Z.), irene.rembado@gmail.com (I.R.), dc342b@nih.gov (D.C.), fetz@uw.edu (E.E.F.)
https://doi.org/10.1016/j.cub.2018.07.009

SUMMARY

The functional role of cortical beta oscillations, if any, remains unresolved. During oscillations, the periodic fluctuation in excitability of entrained cells modulates transmission of neural impulses and periodically enhances synaptic interactions. The extent to which oscillatory episodes affect activity-dependent synaptic plasticity remains to be determined. In nonhuman primates, we delivered single-pulse electrical cortical stimulation to a "stimulated" site in sensorimotor cortex triggered on a specific phase of ongoing beta (12–25 Hz) field potential oscillations recorded at a separate "triggering" site. Corticocortical connectivity from the stimulated to the triggering site as well as to other (non-triggering) sites was assessed by cortically evoked potentials elicited by test stimuli to the stimulated site, delivered outside of oscillatory episodes. In separate experiments, connectivity was assessed by intracellular recordings of evoked excitatory postsynaptic potentials. The conditioning paradigm produced transient (1–2 s long) changes in connectivity between the stimulated and the triggering site that outlasted the duration of the oscillatory episodes. The direction of the plasticity effect depended on the phase from which stimulation was triggered: potentiation in depolarizing phases, depression in hyperpolarizing phases. Plasticity effects were also seen at non-triggering sites that exhibited oscillations synchronized with those at the triggering site. These findings indicate that cortical beta oscillations provide a spatial and temporal substrate for short-term, activity-dependent synaptic plasticity in primate neocortex and may help explain the role of oscillations in attention, learning, and cortical reorganization.

INTRODUCTION

Activity-dependent synaptic plasticity is a fundamental mechanism for the shaping of cortical neuronal circuits during development [1], their modification with learning [2], and their reorganization after neural injury [3]. The strength of synaptic connections can be modulated by the relative timing of presynaptic and postsynaptic activity: synapses are strengthened (or weakened) when the presynaptic neuron fires before (or after) the postsynaptic neuron (e.g., [4]).

Cell activity in the sensorimotor (SM) cortex of nonhuman primates can be entrained with beta oscillations (12–25 Hz) of the extracellular field potential [5, 6]. Neurons typically fire at higher rates during the depolarizing (surface-negative) phase and at lower rates during the hyperpolarizing phase [6–8]. *In vivo* intracellular recordings confirm that subthreshold membrane potentials exhibit waves of depolarization synchronized with the field potentials [7] (Figure 1B). Temporal relations among the oscillatory activities of populations of interconnected cells should influence synaptic plasticity: cells entrained with oscillatory cycles tend to fire in phase with each other, which would favor synaptic potentiation, whereas cells that fire out of phase would favor synaptic depression. This dependence of synaptic plasticity on relative timing with oscillatory neuronal activity has been suggested on theoretical grounds [1, 9, 10] and demonstrated in cortical synapses *in vitro* [11] and in the hippocampus *in vivo* [12]. The time course, detailed phase dependence, and cortical extent of these effects in the neocortex remain unknown.

Neocortical beta oscillations occur "spontaneously" and in relation to many behavioral conditions, including selective attention and working memory [5, 13–17] and motor skill learning [18, 19], for which attention is a prerequisite. The network mechanisms underlying attention and skill learning remain to be understood, but cortical plasticity effects are essential for both, in theoretical and computational models [10, 18–22]. For example, it has been suggested that oscillations shape the spatiotemporal patterns of neural activity in an efficient way that, in short timescales, promotes short-term plasticity that facilitates attentional selection of particular stimuli or actions [23] and, over longer timescales, promotes long-term plasticity needed for skill learning [10]. A recent study in humans showed that the amplitude of alpha and beta oscillations modulates the corticocortical-evoked responses [24]. However, an association between oscillations and synaptic plasticity has not been demonstrated in the neocortex of awake animals.

There is also evidence that oscillations and synaptic plasticity effects in circuits between the motor cortex and the basal

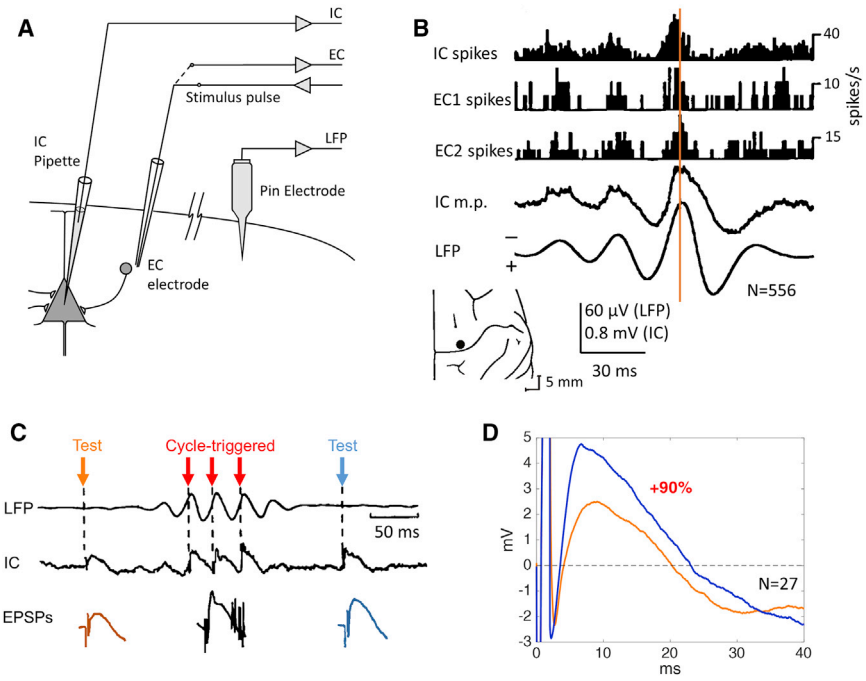

Figure 1. Intracellular and Extracellular Recordings during Cortical Oscillations

(A) Experimental setup. Intracellular (IC) electrode-impaled motor cortex cell and extracellular (EC) electrodes recorded neighboring activity or stimulated presynaptic cells.

(B) Cycle-triggered average aligned with depolarizing phase of EC local field potentials and showing histograms of spikes recorded by IC and EC electrodes and IC membrane potential (m.p.). Inset shows the precentral location of the sites from which the recordings were made.

(C) EPSPs were evoked by cycle-triggered stimuli during the depolarizing phase of oscillatory episodes and by preceding and following test stimuli.

(D) Superposition of averaged EPSPs evoked by pre- and post-episode test stimuli.

ganglia may be involved in the pathophysiology and pathogenesis of Parkinson's disease (PD). For example, cortico-basal oscillatory synchrony in the beta range is abnormally elevated in PD; it correlates with the severity of parkinsonism, and it may contribute to abnormal information transmission between the thalamus and the cortex [25]. In addition, altered levels of synaptic plasticity have been described in both the motor cortex and the basal ganglia in PD, which may be involved in the long-term pathogenesis of the disease, by contributing to the development of abnormal synchrony in cortico-basal circuits [26]. Whether oscillatory synchrony and altered plasticity are interrelated in PD is unknown; the implications of such a relationship would be significant, for both the treatment of parkinsonian symptoms and in long-term therapies for PD.

For these reasons, a direct link between *in vivo* oscillatory activity and synaptic plasticity would have implications for both normal and abnormal cortical states. Several important questions remain unresolved. Do field potential oscillations in the neocortex modulate synaptic transmission in a persistent manner that outlasts the oscillations themselves? If so, what is the duration and spatial extent of plasticity effects produced by widespread oscillations? And is such modulation mediated by spike-timing-dependent synaptic plasticity (STDP) mechanisms?

We addressed these questions using closed-loop cortical stimulation triggered from cycles of oscillatory field potentials recorded from the SM cortex of awake monkeys [27, 28]. The effects of cycle-triggered stimulation in primate cortex were investigated under two conditions: intracellular recordings of evoked excitatory postsynaptic potentials (EPSPs) and epidural recordings of cortically evoked potentials (CEPs). For the latter, we used minimally invasive, epidural electrocorticography (ECoG) electrodes to record ECoG activity at one cortical site (the "triggering site") and to deliver stimuli at a second "stimulated site." The strength of their synaptic connections was measured by the size of the CEPs evoked at the triggering site by test stimuli at the stimulated site (Figure 2). Conditioning was performed by triggering stimuli during a specific phase of the oscillatory cycles at the triggering site. This conditioning produced transient changes in the CEPs that outlast the duration of the oscillatory episodes. The direction of this plasticity effect depends on the oscillatory phase from which stimulation was triggered: potentiation from stimulation during depolarizing phases, depression during hyperpolarizing phases. Effects were also seen at non-triggering sites that exhibited oscillations synchronized with those at the triggering site. These findings indicate that cortical beta oscillations provide a spatial and temporal substrate for short-term, activity-dependent synaptic plasticity in the neocortex. They also suggest that closed-loop electrical stimulation using minimally invasive brain-surface electrodes could be used in neurorehabilitation and in treatment of movement disorders.

RESULTS

Closed-Loop Cortical Stimulation

Modulation of Intracellular EPSPs

Initial experiments were performed in studies of synaptic interactions between primate motor cortex neurons using *in vivo* intracellular (IC) and extracellular (EC) recordings [7, 29]. Simultaneous IC and EC recordings showed that oscillatory local field potential (LFP) episodes were associated with correlated membrane potential fluctuations as well as with entrained EC spikes (Figure 1B). Extracellular stimuli delivered near the IC neuron evoked monosynaptic EPSPs that were tested at low rates of stimulation (Figures 1A and 1B). When a nearby EC electrode detected an episode of field potential oscillations, stimuli were delivered at a specific phase of the oscillatory cycles (Figure 1C). This produced a post-episode increase or decrease of the EPSP amplitude, depending on whether the cycle-triggered stimuli occurred during the depolarizing or the hyperpolarizing phase of the oscillations (Figure 1D). The results for six sessions are plotted by the black points in Figure 3C. These experiments

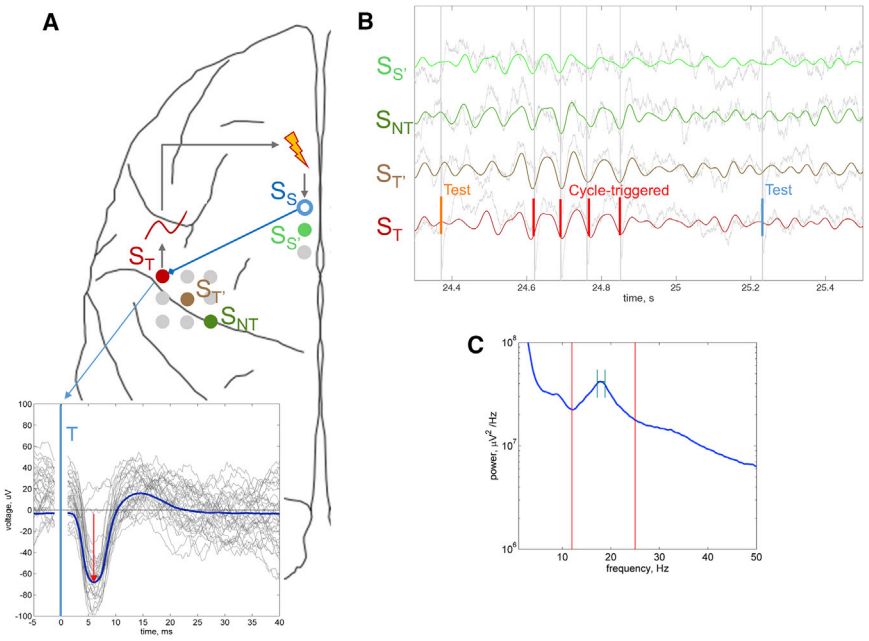

Figure 2. Beta Cortical Oscillations, Closed-Loop Beta Cycle-Triggered Cortical Stimulation, and Cortically Evoked Potentials

(A) Sites in sensorimotor and supplementary motor area in monkey 1. Stimuli at the stimulated site (S_S, open blue circle) elicited cortically evoked potentials at the triggering site (S_T, filled red circle). Inset shows 30 superimposed stimulus-triggered sweeps (gray) and the average of ~600 sweeps (blue). Amplitude of first negative peak was measured (downward red arrow). See also Figure S1.

(B) Spontaneously occurring episodes of ECoG oscillations (band-pass filtered between 12 and 25 Hz), of approximately 18 Hz frequency, recorded at the four selected frontal cortical electrodes shown in (A): site close to the stimulated site (S_S, light green), non-triggering site (S_{NT}, dark green), site close to the triggering site (S_T, brown), and the triggering site (S_T, red). Negative phases triggered stimuli to the stimulated site. When oscillations were not detected for at least 500 ms, test stimuli were delivered to the stimulated site. Black traces show raw recordings; colored traces show filtered records. See also Figure S2.

(C) Average power spectrum of cortical signals recorded from different triggering sites across months of recordings. Red lines show corner frequencies of the beta band-pass filter. Peak beta frequency in this monkey was around 18 Hz (SD of peak frequency, 0.8 Hz [green vertical lines around mean]).

established that oscillatory episodes modulated subsequent synaptic interactions at the cellular level but were difficult to perform in sufficient quantity to fully document the phase dependence and time course of the changes. We therefore examined this phenomenon more systematically at the population level with epidural recording and stimulation.

Establishing Corticocortical Functional Connectivity Using Cortically Evoked Potentials

In monkeys with ECoG arrays, we randomly selected pairs of recording and stimulating sites that had a corticocortical connection. Functional connections between cortical sites were identified in initial experiments by cortically evoked potentials (CEPs), as evidenced by averages of many cortical potential responses at a cortical site elicited by electrical stimulation of another cortical site, delivered as single stimuli at regular intervals (one every 2 s), at a current intensity slightly above (~110%) the threshold for eliciting such responses (2.5–4.5 mA for monkey 1, 0.7–2.5 mA for monkey 2; Figure S1). Pairs of sites with consistent CEPs for three consecutive daily sessions were considered "functionally connected" and were used in the conditioning sessions. The amplitude of the early component of the CEPs probably represents mono- or polysynaptically mediated postsynaptic potentials [30]. We used the amplitude of the earliest resolvable component of the CEP (henceforth, CEP amplitude), typically peaking at 3–7 ms post-stimulus (Figures 2A and S1), as a measure of the overall strength of the synaptic projection from the stimulated to the recording site. Such CEPs were elicited by test stimuli to the stimulated site, delivered at a constant rate of two per second when no oscillatory episodes were detected at the triggering site (Figure 2B).

Occurrence of Cortical Oscillations

Fast cortical oscillations in the "beta" band (12–25 Hz) were recorded from the primary motor (M1) and supplementary motor areas (SMAs) [31] of two awake monkeys using epidural ECoG electrodes (Figure 2A). These oscillations appeared spontaneously when the monkeys were awake and resting quietly in the primate chair, i.e., generating no motor output and getting frequently rewarded for that to ensure that they did not fall asleep. Oscillations typically occurred in episodes of 2–5 oscillatory cycles (Figures 2B and S2). In the neural recordings reported in this study, oscillations were most synchronous to each other within the beta range (Figure S2). Peak beta frequency was approximately 18 Hz for monkey 1 (Figure 2C) and 16.5 Hz for monkey 2 and remained stable throughout the 6-month duration of the study: SD of peak beta frequencies across all experiments was 0.8 Hz for monkey 1 (Figure 2C) and 0.6 Hz for monkey 2. The negative (or positive) phase of these LFP oscillations have been shown to be associated with depolarizing (or hyperpolarizing) potentials recorded *in vivo* [7] and higher (or lower) levels of firing in the local neuronal populations [5, 6] (Figure 1B).

Triggering Stimuli from Oscillations

We used phases of spontaneous cortical oscillations to trigger delivery of stimuli-evoking input to the recording site (e.g., [7]). We extracted the beta component (12–25 Hz) of the signal from a selected triggering cortical site and identified large oscillatory cycles, defined as cycles with amplitude at least 3× SD of a 2- to 3-min-long "baseline" recording from the triggering site. We manually selected a negative (depolarizing) or positive (hyperpolarizing) oscillatory phase of the cycle to trigger electrical stimulation at another site that evoked CEPs at the triggering site (Figure 2A). The time delay introduced by the real-time operation of this loop was measured to be between 3 and 5 ms, depending on oscillatory frequency; this corresponds to a phase shift of approximately 17° at the peak beta frequency of 18 Hz for monkey 1 and 19° at 16 Hz for monkey 2. By delivering

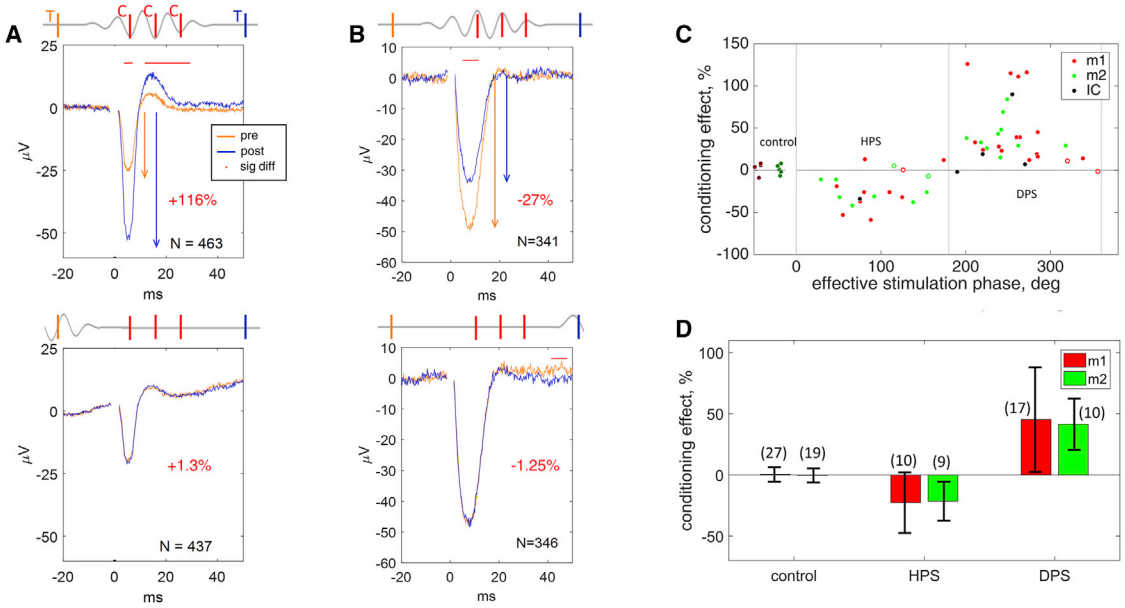

Figure 3. Bidirectional Modification of Cortical Connectivity by Phase-Dependent Stimulation

(A) Depolarizing phase stimulation produces synaptic potentiation. Top: Conditioning stimulation was triggered from the negative (depolarizing) phase of oscillatory beta cycles (red vertical bars, C) and test stimuli (T) were delivered before (orange) and after (blue) conditioning episodes. Cortically evoked potentials (CEPs) elicited by test stimuli were registered at the triggering site. Traces show the average CEP elicited by test stimuli preceding conditioning episodes with at least three cycle-triggered stimuli (orange) and the CEP elicited by test stimuli following the episodes (blue). The amplitude of the first component (downward arrows) of the post-conditioning CEP was 116% larger than that of the pre-conditioning CEP. See also Figure S3. Bottom: Delivering the same sequence of test and cycle-triggered stimuli at a later time in open-loop mode produced no significant changes in the CEP amplitude. For additional controls, see Figure S4.

(B) Hyperpolarizing phase stimulation produces synaptic depression. Top: Post-conditioning episode CEPs was 27% smaller than pre-conditioning episode CEPs. Bottom: No significant changes were seen in CEP amplitude in the control experiment. Red horizontal bars with asterisks indicate the portions of the CEP during which contiguous samples are significantly different in the pre- versus post-conditioning comparison (at the $p = 0.001$ confidence level).

(C) Magnitude of the conditioning effect in individual experiments as a function of the effective stimulation phase (0°–350°). Conditioning effect was defined as the percent change of amplitude between CEPs elicited from test stimuli preceding bursts of three or more cycles and from test stimuli immediately following those bursts. Vertical lines mark 0°, 180°, and 360°. Ten randomly selected data points from control experiments (five from each monkey) are shown to the left of the 0° line. Open circles denote the five experiments in which there were no significant changes in the CEP shapes. Colors show data points obtained from monkey 1 (red), monkey 2 (green), and intracellular recordings (black).

(D) Average magnitude of the conditioning effects. Bars show collective results for three groups of experiments: control, HPS, and DPS. For HPS experiments, the effective mean instantaneous stimulation phase (ISP) was between 0° and 180°, and for DPS, mean ISP was between 180° and 360°. Bars: mean ± SD; numbers: n. of observations in that group. The conditioning effects in closed-loop stimulation experiments were greater than in respective control experiments both for HPS sessions ($p = 0.012$ and $p = 0.037$ for monkey 1 and 2, respectively; paired t test assuming unequal variances) and for DPS sessions ($p < 0.001$ for both monkeys; paired t test assuming unequal variances).

conditioning stimuli during the depolarizing (or hyperpolarizing) phase of oscillatory cycles, we temporally associated a stimulation-elicited synaptic input with a spontaneous depolarizing (or hyperpolarizing) event at the triggering site.

Experimental Timeline

Each conditioning session was performed with the monkey sitting comfortably in a primate chair, inside a recording booth; the animal was kept awake and alert by periodic applesauce rewards for not generating any upper limb movement. A triggering-stimulated site pair was selected, and a baseline series of 500 test stimuli was delivered at the stimulated site at 2/s, while recording from the triggering site as well as from other cortical sites. After manually setting the cycle detection parameters, closed-loop stimulation was performed for 30–40 min, during which time both cycle-triggered and intervening test stimuli were delivered at the stimulated site. At the end of the oscillatory episode, a post-conditioning series of test stimuli was delivered every 500 ms to document the decay of the conditioning effect. Neither test nor conditioning stimuli had any temporal alignment with the delivery of rewards (data not shown).

Phase-Dependent Modification of Corticocortical Connectivity

When closed-loop stimulation was triggered from a negative oscillatory potential at the triggering site (depolarizing-phase stimulation [DPS]), the CEP responses to test stimuli following a conditioning burst were larger than those to test stimuli preceding the burst (Figure 3A, top). This occurred only for conditioning bursts with three or more consecutive cycle-triggered stimuli; bursts with two stimuli were typically not associated with significant changes in CEP amplitude (Figure S3). To control for the possibility that this potentiation could be due to the stimulation sequence itself, we recorded stimulus times, for both test and conditioning stimuli, during each conditioning session and "replayed" that entire stimulus sequence to the same stimulated site at a later time but in open-loop mode, without any

relationship to ongoing cortical activity. These control stimuli produced no evidence for CEP amplitude potentiation (Figure 3A, bottom).

When closed-loop stimulation was triggered from surface-positive oscillatory potentials (hyperpolarizing phase stimulation [HPS]), we observed depression of the CEP response following the conditioning burst (Figure 3B, top). This change was not present in open-loop control conditions (Figure 3B, bottom).

The magnitude and polarity of the conditioned change in CEP is plotted in Figure 3C as a function of phase. This plotted ''effective'' phase is corrected for delays to represent the estimated arrival time of the stimulus-evoked volley. This arrival time can be estimated by the known latency introduced by the closed-loop system (3 ms) and the onset latency of the CEP. The onset latency of the large majority of CEPs was 3–5 ms (Figure S1), for a total arrival time of 6–8 ms. This time corresponds to a phase delay, relative to the triggering phase, of 39°–52° for monkey 1 (peak beta frequency 18 Hz) and 35°–47° for monkey 2 (peak beta frequency 16.5 Hz). This means that when, for example, in monkey 1, stimuli are triggered from the peak of the beta cycle at the stimulated site, at a phase of 90°, the volley of action potentials elicited by a stimulus at the stimulated site reaches the triggering site at an effective phase of 125°–137°. The number of conditioning stimuli had no systematic effect on the latency of CEP (data not shown).

Overall, DPS was associated with an average increase in CEP amplitude of about 45% in monkey 1 and 38% in monkey 2. In contrast, HPS was associated with an average decrease of CEP amplitude of 28% in monkey 1 and 24% in monkey 2 (Figures 3C and 3D).

The magnitude of the conditioning effect did not depend on the distance between the triggering and the stimulated sites (Figure S5). Interestingly, in both animals, sessions in which there was smaller variability in the instantaneous oscillatory phase at which conditioning stimuli were delivered, as quantified by the SD of the instantaneous stimulation phase distribution at the triggering site, were associated with larger CEP amplitude changes (Figures 5A and 5C). In other words, when conditioning stimuli were delivered, and the evoked volleys arrived at the triggering site, at a more consistent phase (either depolarizing or hyperpolarizing) from cycle to cycle, the conditioning effect at that site was stronger. This effect was present in the triggering as well as the non-triggering sites and is discussed further below.

To test the possibility that oscillatory activity alone might be associated with CEP amplitude changes that persist beyond the duration of oscillations, we performed separate control experiments in which no conditioning stimuli were delivered during oscillatory episodes. Test stimuli delivered immediately before and after oscillatory episodes revealed no changes in CEP amplitudes, indicating that oscillatory activity alone did not produce the observed effects (Figure S4).

We found no indication that triggering conditioning stimuli from oscillatory activity in the low gamma range had similar conditioning effects in either animals. In four experiments conducted in each of the two animals, in which conditioning stimuli were triggered from depolarizing phases of low gamma (25–40 Hz) oscillations, the change in CEP size between pre- and post-stimulus test pulses ranged between 0.7% and 4.3%.

Duration of the Plasticity Effect

Delivering test pulses every 500 ms after the end of oscillatory episodes revealed the time course of conditioned changes in CEP amplitude as a function of delay after conditioning. We observed that amplitudes of responses to consecutive test stimuli progressively returned to pre-conditioning levels in both DPS (Figure 4A) and HPS experiments (Figure 4B). With DPS, the potentiation effect lasted for up to 2 s after the end of conditioning (Figure 4C), whereas with HPS, the depression effect lasted up to 1.5 s (Figure 4D).

To test whether conditioning sessions also had a cumulative longer-lasting effect on cortical connectivity, we compared CEP responses from 500 test stimuli delivered before the beginning of each conditioning (or control) stimulation session to those from 500 test stimuli delivered after it. When closed-loop stimulation produced longer-term CEP changes, those were no different than with corresponding control stimulation condition (data not shown), suggesting that those changes were a nonspecific cumulative effect of electrical stimulation, compatible with stimulation-induced change in neuronal excitability [32] and not a long-term manifestation of Hebbian plasticity. This nonspecific stimulation effect on CEP amplitude was inversely related to the distance between the stimulated and the triggering sites, which further differentiated it from the short-term Hebbian plasticity effects (Figure S5).

Connectivity Changes at Non-triggering Sites

Stimuli delivered at the stimulated site often evoked CEPs not only at the triggering site but also at other cortical sites. Some of those other sites also had oscillatory potentials associated with those in the triggering site but with different degrees of phase difference and cycle-to-cycle phase coherence. A site at which oscillations occur in tighter synchrony with the triggering site would have an instantaneous oscillatory phase closer to that of the triggering site when conditioning stimuli were delivered. The resulting instantaneous stimulation-phase difference between the triggering and a non-triggering site was generally greater with increasing distance between the two sites (data not shown), as previously documented [8]. The variability of instantaneous stimulation phase (ISP) at a cortical site was minimal at the triggering site and increased with increasing distance from it (Figure S6). We found conditioning-related CEP changes at non-triggering sites, but those were typically smaller than CEP changes at the triggering site (Figures 5A and 5B). The magnitude of the connectivity change at a non-triggering site was inversely proportional to the ISP variability associated with that site, as quantified by the SD of the ISP distribution (Figure 5C). No clear relationship was evident between the magnitude of the conditioning effect on non-triggering sites and the mean absolute difference in ISP between those and the triggering site (data not shown).

DISCUSSION

Our study provides direct neurophysiological evidence for a role of fast, beta range (12–25 Hz) cortical oscillations in the modulation

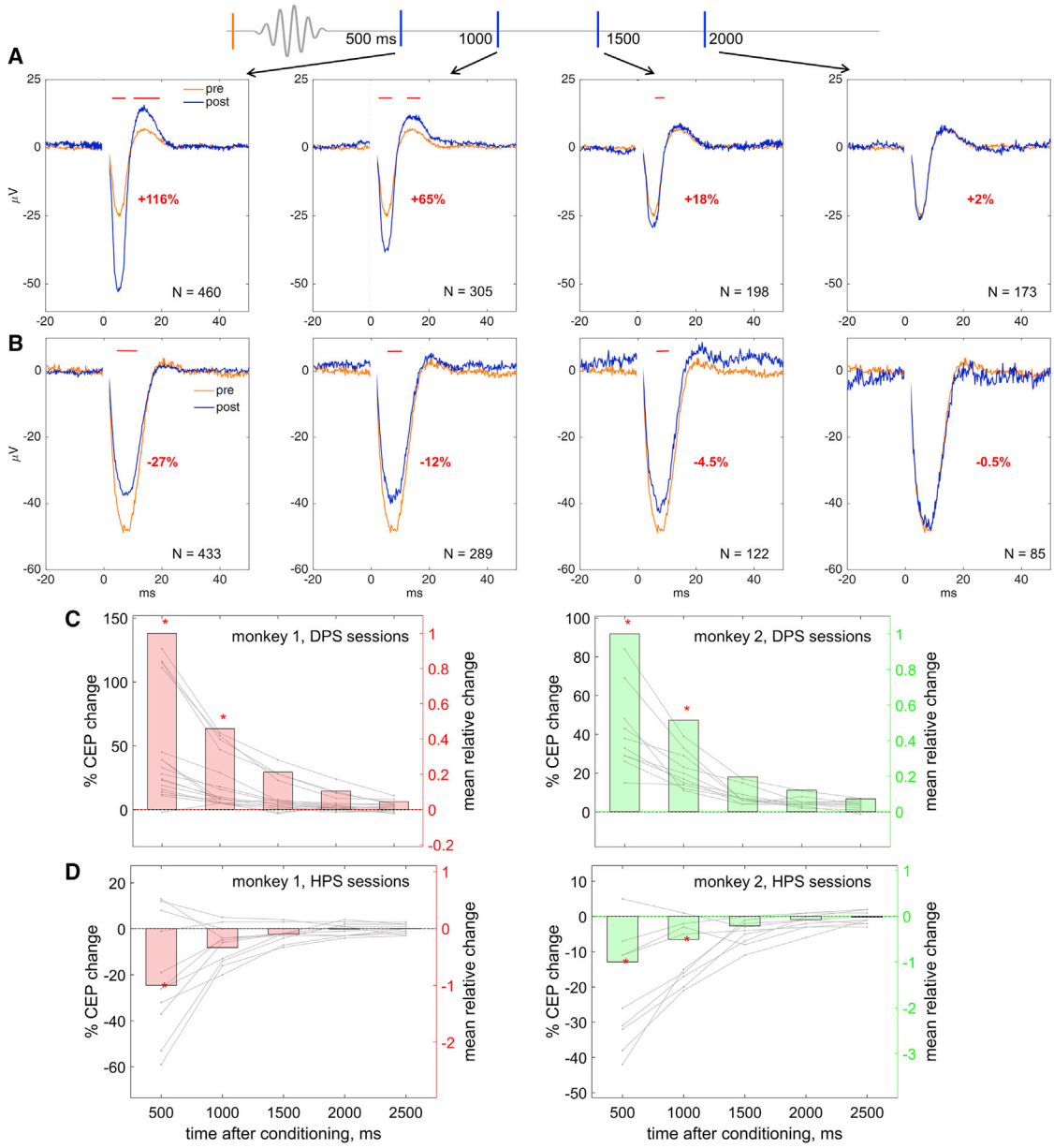

Figure 4. Time Course of the Conditioning Effect

(A) Time course of the conditioning effect in a DPS experiment. Average CEPs for successive test stimuli delivered every 500 ms (top). Red horizontal bars indicate segments of the CEP during which all samples are significantly different in the pre- versus post-conditioning comparison ($p < 0.001$). The percentages give the degree of potentiation (positive) or depression (negative), quantified by the relative change in the CEP amplitude from the pre-conditioning level.

(B) Time course of conditioning effect in a HPS experiment.

(C and D) Overall time course of conditioning effect in all triggering sites. Panels show change in CEP amplitude (relative to pre-conditioning test stimulus) as a function of time after the last pulse of the conditioning burst. Dots connected by gray lines are measurements from single experimental sessions. Colored bars are the mean CEP change relative to the change at 500 ms post-conditioning for that time point, across all sessions (right axis). Red asterisks denote times at which CEP change, relative to pre-conditioning, was significantly different than 0, at the 0.05 significance level.

of synaptic plasticity in awake primates. Under closed-loop conditions, we associated bursts of depolarizing or hyperpolarizing oscillatory field potentials at a cortical site with stimulation-elicited activation from another. This conditioning paradigm produced a short-lived (1.5–2 s) modification of functional connectivity between the two sites that outlasted the oscillatory episodes and exhibited a bidirectional phase dependence: potentiation for depolarizing phases or depression for hyperpolarizing phases.

Neural Mechanism Mediating the Conditioning Effect

In principle, the conditioned change in CEP amplitude could be related to three possible mechanisms: it could reflect a change

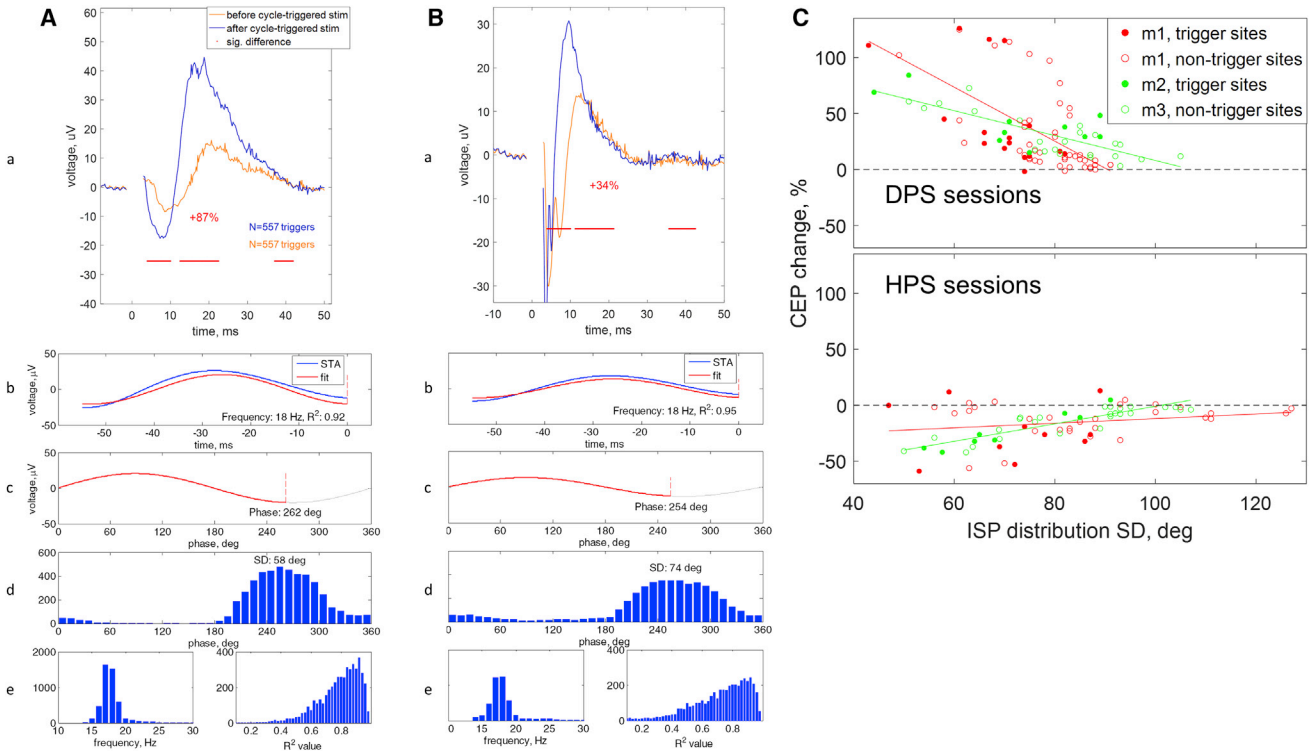

Figure 5. Conditioning Effects in Triggering and Non-triggering Sites

(A) Conditioning effect and stimulation phase at the triggering site. (a) Effect of DPS conditioning. (b) Stimulus-triggered average (STA) of raw ECoG (blue) and sinusoidal fit (red line) compiled from conditioning stimuli, in a DPS experiment in monkey 1. Time 0 corresponds to the delivery of the conditioning stimulus. Oscillatory frequency was estimated by fitting a sinusoid to the STA; it was 18 Hz, with an R^2 value of 0.92. (c) Mean oscillatory phase at the time of stimulation, estimated from the STA, was 262° (d) Distribution of phases at the time of all individual conditioning stimuli in this session; ISP values were estimated by fitting a sinusoid to individual sweeps preceding individual conditioning stimuli. The SD of the ISP distribution is 58°. (e) Left: Distribution of estimated instantaneous frequency values for all conditioning stimuli; average was 18 Hz. Right: Distribution of R^2 values, indicating goodness of fit, for sinusoidal fit of individual sweeps. (B) Stimulation phase and conditioning effect at a non-triggering site. Rows and panels correspond to those in (A). The effect of conditioning on this site was smaller than that at the triggering site: CEP increased by 34%. The SD of the ISP distribution at this site (74°) was larger than that at the triggering site.

(C) Dependency of the conditioning effect on the SD of the ISP distribution at all triggering (filled symbols) and non-triggering sites (open symbols) in monkey 1 (red symbols) and monkey 2 (green symbols), separately for DPS (top) and HPS experiments (bottom). Conditioning effect is expressed as % CEP amplitude change. The colored lines represent the linear regression lines for monkey 1 and monkey 2 (red and green, respectively). In general, the larger the SD of the ISP distribution at a cortical site, the smaller the conditioning effect at that site (% CEP change approaches 0).

Correlation coefficients between % CEP change and SD of ISP distribution in the DPS experiments were 0.61 and −0.79 for monkey 1 and monkey 2, respectively ($p < 0.01$ in both cases), and in the HPS experiments 0.22 and 0.88 for monkey 1 and monkey 2, respectively ($p = 0.18$ and $p < 0.01$).

See also Figures S5 and S6.

in the strength of the synaptic projection from the stimulated to the triggering site, a change in the excitability of cells at the stimulated site, or a change in the excitability of cells at the triggering site (Figure 6). In the first case, the same stimulus-evoked presynaptic volley would generate an altered postsynaptic response via a change in synaptic connection (Figure 6A). In the second, the same stimulus would elicit a larger (or smaller) presynaptic volley, and consequently an altered postsynaptic response, without synaptic modification (Figure 6B). In the third case, the same presynaptic volley would generate an altered postsynaptic response, without synaptic modification, because the same synaptic action would elicit larger (or smaller) activation of more (or fewer) excitable postsynaptic cells (Figure 6C). These scenarios can be further resolved by considering the effects at the non-triggering sites.

A change in the excitability of the stimulated site would have similar effects on the CEP at the triggering site and the non-triggering sites. However, in many cases, the non-triggering sites showed no change in the CEP. When the non-triggering sites did show changes in the CEP, the magnitude of these changes was smaller than those at the triggering site and was dependent on phase differences. This differential effect cannot be explained by a possibly larger projection from the stimulated site preferentially to the triggering site, because the latter was chosen randomly among all sites "receiving" CEPs from the stimulated site.

Could the conditioning effect be mediated by a change in the post-conditioning excitability of the triggering site? Such an effect could be produced either by a direct or by a synaptically mediated effect of stimulation on the triggering site. The first possibility is unlikely, as there was no inverse relationship between the conditioning effect and the separation between stimulated and triggering site (Figure S5). Interestingly, in DPS experiments in monkey 1, longer distances to the stimulated

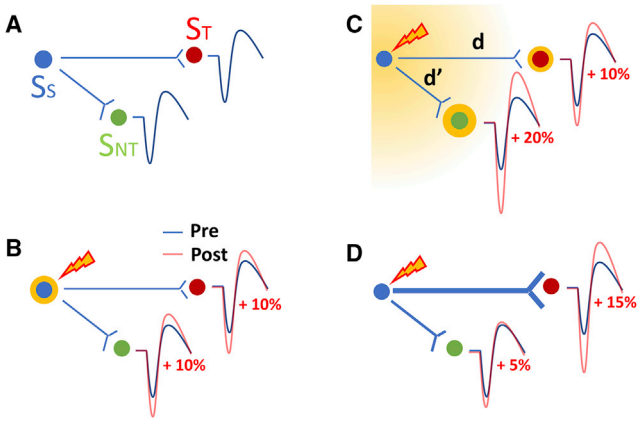

Figure 6. Possible Mechanisms for the Conditioning Effect

Schematic representation of three scenarios that could explain the conditioning effect.

(A) Diagram of the cortical circuit undergoing conditioning. The triggering site (S_T), from which oscillations are recorded, receives a cortical connection from the stimulated site (S_S), manifesting as a cortically evoked potential (CEP), shown with blue trace. A non-triggering site (S_{NT}) also receives a connection from S_S and undergoes oscillations in phase with those at S_T.

(B) Scenario 1: Stimulation of S_S leads to stimulation phase-dependent change in the excitability of S_S, in this case an increase with depolarizing phase stimulation (DPS). This would result in uniform relative change in the size of CEPs in both S_T and S_{NT}, since both CEPs are elicited by stimulation of a now more excitable S_S.

(C): Scenario 2: Stimulation of the S_S leads to a change in the excitability of both S_T and S_{NT} dependent on stimulation phase and distance. This would result in a larger change in the size of CEPs in the site that is closer to S_S because of current spread.

(D): Scenario 3: Stimulation of the S_S leads to phase-dependent modification of the connectivity from S_S to both S_T and S_{NT}, consistent with spike-timing-dependent plasticity. This would result in a larger change in the size of CEPs at the S_T than at the S_{NT} because of tighter correlation of the phase of oscillatory activity at S_T with the stimulation-elicited volley from S_S.

site were associated with greater conditioning changes, due to the preponderance of strong potentiation effects between M1 and SMA sites (Figure S5, points surrounded by circle). Conditioning effects were seen at long (>15 mm) distances between the stimulated and the triggering sites, but direct effects of cortical stimulation were not seen at distances beyond 10 mm from the stimulated site (Figure S5), consistent with other experimental and theoretical studies [33, 34]. The second possibility requires that CEPs change more at sites that receive a larger projection from the stimulated site. The conditioning effect at the triggering site was typically larger than the effects at non-triggering sites, even though the triggering site did not necessarily receive a larger projection from the stimulated site, since it was chosen randomly (Figure 5).

Thus, the most likely mechanism producing the effect of conditioning stimulation on CEPs is synaptic modification. When presynaptic activity is triggered by, and therefore coincides with, postsynaptic depolarization, transient synaptic potentiation occurs; when presynaptic activity coincides with relative postsynaptic hyperpolarization, synaptic depression occurs. These findings are consistent with a Hebbian-like plasticity mechanism. The dependence of the direction of synaptic modification—potentiation or depression—on the level of postsynaptic depolarization has been demonstrated in both the hippocampus [35, 36] and the neocortex [37, 38] and has been postulated to include STDP as a special case [39].

In our study, synaptic potentiation effects were stronger than depression effects in both animals. Part of that difference may be explained by possible correlated oscillations at the stimulated site. Thus, in DSP sessions, conditioning stimuli would be delivered when local cells were depolarized, resulting in a larger evoked presynaptic volley and, therefore, greater plasticity effect. In HSP sessions, stimuli would be delivered at a hyperpolarized phase, producing a smaller stimulus-evoked volley and smaller plasticity effect. This explanation assumes that the stimulated and the triggering site potentials were at similar depolarization levels during conditioning stimulation (e.g., Figure 2B). The absolute difference in the ISP between the triggering site and any other site, including the stimulated site, ranged between 0° and 30° (data not shown), and the beta coherence between the triggering site and other sites was generally above 0.9 (Figure S2), suggesting that was generally the case.

Typically, for a given triggering phase, the maximal connectivity change, and therefore synaptic modification, occurred between the stimulated and the triggering sites. This is expected, since neural activity at the triggering site is most tightly synchronized with stimulus-evoked activation and a tight coincidence between pre- and postsynaptic activity is a critical factor for synaptic modification [4]. However, connectivity changes also occurred between the stimulated and non-triggering sites showing CEPs (Figure 5). This is also expected, because oscillatory episodes at most of those sites were in phase with those at the triggering site. However, the temporal relationship of conditioning stimuli with oscillatory phase at non-triggering sites was more variable than with the triggering site, so stimulus-evoked presynaptic volleys arrived at non-triggering sites over a wider range of postsynaptic depolarization levels. That would explain why changes in connectivity between stimulated and non-triggering sites were generally smaller than those between stimulated and triggering sites.

Induction and Duration of Synaptic Modification

Induction of both long-term potentiation (LTP) and depression (LTD), the two classic forms of synaptic plasticity, requires a large number and/or high frequency of presynaptic-postsynaptic pairings (e.g., [38]). We found that three or more consecutive conditioning stimuli (Figure S3), at an average frequency of about 20 Hz, were sufficient to induce short-term potentiation or depression. We could not measure directly the magnitude of neuronal activation by each stimulus, but a large number of action potentials are probably elicited. A volley of many presynaptic action potentials arriving at the postsynaptic site nearly simultaneously could, through temporal summation, mimic short, high-frequency stimulation trains that are effective at producing synaptic changes in *in vitro* models (e.g., [35, 40, 41]). Although it is conceivable that the phase of the first conditioning stimulus in a burst is critical for the plasticity effect, the remainder are also necessary, as evidenced by the effect of cycle number and phase variance on the magnitude of conditioned effects.

Both LTP and LTD produced by longer conditioning protocols typically last minutes to days [42], much longer than the

conditioning effect observed in this study (1.5–2 s) (Figure 4). Short-lived synaptic modification occurred when brief trains of impulses (2–40) were delivered at moderate or high frequencies (20–400 Hz); the synaptic modification was dependent on postsynaptic NMDA receptor (NMDAR) activation and declined very rapidly, within a few seconds to a few minutes, after its induction (e.g., [31, 35, 41]). It should be noted that the CEP measure used in the present study reflects events produced by a large population of synapses. Given the variety of short- and long-term synaptic plasticity processes that co-exist in a population of diverse synapses, this population response likely reflects a mixture of synaptic potentiation and depression with different induction and decay kinetics.

The short-lived synaptic modification we describe here could represent an early phase of LTP that stabilizes when additional conditions are met [43]. It has been suggested that these additional conditions may come into play in the context of reinforcement learning [44–48]. According to this theory, a set of synapses undergo short-term plasticity during coordinated neuronal activity associated with a sensory stimulus, an action, or a brain state. A delayed reward signal may then, through neuromodulatory action, select which of these ''tagged'' synapses are eligible for longer-term changes, on the basis of their plasticity decay kinetics and other factors [49–51]. Recent experiments provided evidence for such a brief ''eligibility trace'' in individual synapses undergoing plasticity in the visual cortical slice [48]. In our study, rewards were delivered independently of oscillatory activity or cortical stimulation; operant conditioning of oscillations in conjunction with activity-dependent cortical stimulation could be used to directly test these assumptions [52].

Physiological and Clinical Implications

Several lines of evidence suggest that cortical oscillations are not mere epiphenomena of cortical organization but play an important role in information processing and computation [14, 52–54], neuronal communication within and across cortical networks [54–56], and modulation of synaptic transmission [7, 57]. Our findings have implications for the role of oscillations in normal cortical function and, potentially, in some brain disorders.

Evidence for a possible role of oscillations in synaptic plasticity has been described in mammalian synapses, e.g., in layer II/III of the rat visual cortical slice [11] and in the CA3-CA1 synapse of the rat hippocampus [12]. Injecting intracellular sinusoidal current paired with phase-locked EPSPs, Wespatat et al. [11] found that prolonged pairings produced LTD in most cases; LTP occurred in half of the pairings with the depolarizing phase. Those studies showed that local oscillatory synchrony may be a determining factor for plasticity at the cortical microcircuit level. Our study shows that such a bidirectional effect is also present within and between widely separated cortical areas in awake primates. This suggests that large-scale oscillatory synchrony may be an important factor for neural communication and also for shaping the strength of long-range corticocortical connections that mediate it. Furthermore, our finding that ECoG oscillations, which reflect coherent aggregate activity of large numbers of neurons, could be involved in large-scale synaptic plasticity effects has important implications for the effectiveness of population activity-based electrical, magnetic, and sensory brain stimulation paradigms [58-61] and neurofeedback therapies [62]. The fact that beta oscillatory signals are an effective cortical signal for use with closed-loop brain-computer interface (BCI) applications is important for the design of clinical BCI systems, as lower frequencies can be recorded more dependably with minimally invasive probes (ECoG and EEG electrodes) than higher-frequency components of cortical activity.

Attention, Working Memory, and Plasticity

Our results pose constraints on how oscillatory coherence across sites could affect synaptic plasticity: neural activity in phase with depolarizing oscillatory cycles would promote synaptic potentiation, whereas out-of-phase activity would promote synaptic depression. It has been theorized that synaptic plasticity, especially short-term plasticity, in recurrent cortical networks is a supporting mechanism for attentional selection of stimulus access to working memory [20–22]. According to this model, rapid and short-lived activity-dependent synaptic changes may facilitate the formation of dynamic, reverberating functional assemblies between cells that ''encode'' behaviorally related features of an attended stimulus [23, 63–65]. The direction and magnitude of these synaptic changes will depend on the temporal coincidence between oscillatory cell activities: synaptic potentiation for in-phase activities, depression for out-of-phase activities. Beta oscillations are ubiquitous in many cortical areas [56, 66], and by grossly reflecting, and possibly affecting, the timing of single cell activity, they may affect the dynamics and spatial distribution of these synaptic changes. Indeed, there is ample evidence for the involvement of beta oscillations and beta coherence in attentional mechanisms [13, 14, 17, 53, 67, 68] and memory formation [69], both of which depend on cortical plasticity. Whether the dynamic neuronal assemblies that have been ''selected'' by attentional mechanisms will gain access to working memory and eventually long-term memory depends on other top-down influences and reinforcement signals [22, 67, 69, 70].

Parkinson's Disease

PD is characterized by pathologically elevated beta oscillations in the cortico-basal ganglia loop [25]. PD is also associated with abnormal levels of motor cortical and basal ganglia synaptic plasticity, both LTP and LTD, that correlate with disease severity and treatment status, in animal models and human subjects [26]. Loss of substantia nigra dopaminergic neurons may be the common enabling event for both abnormalities. The depletion of dopamine in the nigrostriatal pathway ''releases'' the corticostriatal glutamergic synapse, increasing spontaneous activity of striatal neurons, which ultimately exerts an abnormally high excitatory drive to the motor cortex via thalamocortical projections. The characteristic frequency of this cortico-basal loop is within the beta range, and it is feasible that oscillatory beta activity and activity-dependent plasticity, in the striatum and/or the motor cortex, are driving each other during the progression of PD [25]. Our findings provide a mechanistic model for how pathologically elevated beta oscillations could modulate plasticity effects in the motor cortex, further exacerbating PD pathophysiology. They also suggest that cortical or deep brain stimulation triggered from hyperpolarizing phases of beta oscillatory bursts, by promoting synaptic depression, may be an intervention for treating PD symptoms [71, 72], for increasing the efficacy of therapy [73], and possibly for altering the disease progression itself.

Concluding Comments

We have demonstrated that phase-locked stimulation synchronized with beta band oscillations produced modifications of functional connectivity between two sites in the somatosensory cortex of nonhuman primates. Our findings provide direct experimental evidences of the cortical plasticity mechanisms underlying attention and working memory, and they also have implications for disease states associated with abnormal cortical oscillations. Therefore, brain stimulation triggered by beta oscillatory bursts may become a protocol to artificially induce coupling or decoupling of behaviorally relevant brain rhythms between cortical regions with implication in cognitive performance, as well as an intervention for treating neurological diseases.

STAR★METHODS

Detailed methods are provided in the online version of this paper and include the following:

- KEY RESOURCES TABLE
- CONTACT FOR REAGENT AND RESOURCE SHARING
- EXPERIMENTAL MODEL AND SUBJECT DETAILS
- METHOD DETAILS
  - Intracellular recordings
  - Subjects and behavioral task
  - Surgical procedures and implant
  - Recordings
  - Electrical stimulation
  - Closed-loop stimulation
  - Experimental timeline
  - Estimation of phase shift introduced by the BCI
- QUANTIFICATION AND STATISTICAL ANALYSIS
  - Cortically-evoked potentials
  - Estimation of stimulation phase
- DATA AND SOFTWARE AVAILABILITY

SUPPLEMENTAL INFORMATION

Supplemental Information includes six figures and can be found with this article online at https://doi.org/10.1016/j.cub.2018.07.009.

ACKNOWLEDGMENTS

The authors would like thank Larry Shupe for programming assistance and Rebekah Schaefer and Olivia Robinson for assistance with animals. This work was supported by the National Institutes of Health (NS12542 and RR 00166).

AUTHOR CONTRIBUTIONS

S.Z., D.C., and E.E.F. conceived the idea and designed the experiments. S.Z., I.R., and others collected the data. S.Z., I.R., and others analyzed the data. S.Z., I.R., and E.E.F. wrote the paper.

DECLARATION OF INTERESTS

The authors declare no competing interests.

Received: September 22, 2017
Revised: April 4, 2018
Accepted: July 4, 2018
Published: August 9, 2018

REFERENCES

1. Uhlhaas, P.J., Roux, F., Rodriguez, E., Rotarska-Jagiela, A., and Singer, W. (2010). Neural synchrony and the development of cortical networks. Trends Cogn. Sci. *14*, 72–80.
2. Sanes, J.N., and Donoghue, J.P. (2000). Plasticity and primary motor cortex. Annu. Rev. Neurosci. *23*, 393–415.
3. Nudo, R. (2014). Plasticity of cerebral motor functions: implications for repair and rehabilitation. In Textbook of Neural Repair and Rehabilitation, 2e, *Volume 1*, M.E. Selzer, S. Clarke, L.G. Cohen, G. Kwakkel, and R.H. Miller, eds. (Cambridge, UK: Cambridge University Press), pp. 99–113.
4. Feldman, D.E. (2012). The spike-timing dependence of plasticity. Neuron *75*, 556–571.
5. Donoghue, J.P., Sanes, J.N., Hatsopoulos, N.G., and Gaál, G. (1998). Neural discharge and local field potential oscillations in primate motor cortex during voluntary movements. J. Neurophysiol. *79*, 159–173.
6. Murthy, V.N., and Fetz, E.E. (1996). Oscillatory activity in sensorimotor cortex of awake monkeys: synchronization of local field potentials and relation to behavior. J. Neurophysiol. *76*, 3949–3967.
7. Chen, D. (1993). Synaptic interactions between primate cortical neurons revealed by in vivo intracellular potentials (University of Washington), PhD thesis.
8. Murthy, V.N., and Fetz, E.E. (1992). Coherent 25- to 35-Hz oscillations in the sensorimotor cortex of awake behaving monkeys. Proc. Natl. Acad. Sci. USA *89*, 5670–5674.
9. Baroni, F., and Varona, P. (2010). Spike timing-dependent plasticity is affected by the interplay of intrinsic and network oscillations. J. Physiol. Paris *104*, 91–98.
10. Masquelier, T., Hugues, E., Deco, G., and Thorpe, S.J. (2009). Oscillations, phase-of-firing coding, and spike timing-dependent plasticity: an efficient learning scheme. J. Neurosci. *29*, 13484–13493.
11. Wespatat, V., Tennigkeit, F., and Singer, W. (2004). Phase sensitivity of synaptic modifications in oscillating cells of rat visual cortex. J. Neurosci. *24*, 9067–9075.
12. King, C., Henze, D.A., Leinekugel, X., and Buzsáki, G. (1999). Hebbian modification of a hippocampal population pattern in the rat. J. Physiol. *521*, 159–167.
13. Egner, T., and Gruzelier, J.H. (2004). EEG biofeedback of low beta band components: frequency-specific effects on variables of attention and event-related brain potentials. Clin Neurophysiol. *115*, 131–139.
14. Lundqvist, M., Rose, J., Herman, P., Brincat, S.L., Buschman, T.J., and Miller, E.K. (2016). Gamma and Beta Bursts Underlie Working Memory. Neuron *90*, 152–164.
15. Murthy, V.N., and Fetz, E.E. (1996). Synchronization of neurons during local field potential oscillations in sensorimotor cortex of awake monkeys. J. Neurophysiol. *76*, 3968–3982.
16. Watanabe, H., Takahashi, K., Nishimura, Y., and Isa, T. (2014). Phase and magnitude spatiotemporal dynamics of beta oscillation in electrocorticography (ECoG) in the monkey motor cortex at the onset of 3D reaching movements. Conf Proc IEEE Eng Med Biol Soc. *2014*, 5196–5199.
17. Womelsdorf, T., and Fries, P. (2006). Neuronal coherence during selective attentional processing and sensory-motor integration. J. Physiol. Paris *100*, 182–193.
18. Hikosaka, O., Nakamura, K., Sakai, K., and Nakahara, H. (2002). Central mechanisms of motor skill learning. Curr. Opin. Neurobiol. *12*, 217–222.
19. Pineda, J.A. (2005). The functional significance of mu rhythms: translating "seeing" and "hearing" into "doing". Brain Res. Brain Res. Rev. *50*, 57–68.
20. Deco, G., Rolls, E.T., and Romo, R. (2010). Synaptic dynamics and decision making. Proc. Natl. Acad. Sci. USA *107*, 7545–7549.
21. Fiebig, F., and Lansner, A. (2017). A Spiking Working Memory Model Based on Hebbian Short-Term Potentiation. J. Neurosci. *37*, 83–96.

22. Jääskeläinen, I.P., Ahveninen, J., Andermann, M.L., Belliveau, J.W., Raij, T., and Sams, M. (2011). Short-term plasticity as a neural mechanism supporting memory and attentional functions. Brain Res. *1422*, 66–81.
23. Mongillo, G., Barak, O., and Tsodyks, M. (2008). Synaptic theory of working memory. Science *319*, 1543–1546.
24. Usami, K., Milsap, G.W., Korzeniewska, A., Collard, M.J., Wang, Y., Lesser, R.P., Anderson, W.S., and Crone, N.E. (2018). Cortical Responses to Input From Distant Areas are Modulated by Local Spontaneous Alpha/Beta Oscillations. Cereb. Cortex. https://doi.org/10.1093/cercor/bhx36.
25. Stein, E., and Bar-Gad, I. (2013). β oscillations in the cortico-basal ganglia loop during parkinsonism. Exp. Neurol. *245*, 52–59.
26. Udupa, K., and Chen, R. (2013). Motor cortical plasticity in Parkinson's disease. Front. Neurol. *4*, 128.
27. Zanos, S., Richardson, A.G., Shupe, L., Miles, F.P., and Fetz, E.E. (2011). The Neurochip-2: an autonomous head-fixed computer for recording and stimulating in freely behaving monkeys. IEEE Trans Neural Syst Rehabil Eng *19*, 427–435.
28. Rembado, I., Zanos, S., and Fetz, E.E. (2017). Cycle-Triggered Cortical Stimulation during Slow Wave Sleep Facilitates Learning a BMI Task: A Case Report in a Non-Human Primate. Front. Behav. Neurosci. *11*, 59.
29. Matsumura, M., Chen, D., Sawaguchi, T., Kubota, K., and Fetz, E.E. (1996). Synaptic interactions between primate precentral cortex neurons revealed by spike-triggered averaging of intracellular membrane potentials in vivo. J. Neurosci. *16*, 7757–7767.
30. Keller, C.J., Honey, C.J., Mégevand, P., Entz, L., Ulbert, I., and Mehta, A.D. (2014). Mapping human brain networks with cortico-cortical evoked potentials. Philos. Trans. R. Soc. Lond. B Biol. Sci. *369*, 20130528.
31. Erickson, M.A., Maramara, L.A., and Lisman, J. (2010). A single brief burst induces GluR1-dependent associative short-term potentiation: a potential mechanism for short-term memory. J. Cogn. Neurosci. *22*, 2530–2540.
32. McCreery, D.B., Yuen, T.G., Agnew, W.F., and Bullara, L.A. (1997). A characterization of the effects on neuronal excitability due to prolonged microstimulation with chronically implanted microelectrodes. IEEE Trans. Biomed. Eng. *44*, 931–939.
33. Nathan, S.S., Sinha, S.R., Gordon, B., Lesser, R.P., and Thakor, N.V. (1993). Determination of current density distributions generated by electrical stimulation of the human cerebral cortex. Electroencephalogr. Clin. Neurophysiol. *86*, 183–192.
34. Rosenthal, J., Waller, H.J., and Amassian, V.E. (1967). An analysis of the activation of motor cortical neurons by surface stimulation. J. Neurophysiol. *30*, 844–858.
35. Hanse, E., and Gustafsson, B. (1992). Postsynaptic, but not presynaptic, activity controls the early time course of long-term potentiation in the dentate gyrus. J. Neurosci. *12*, 3226–3240.
36. Wigström, H., and Gustafsson, B. (1986). Postsynaptic control of hippocampal long-term potentiation. J. Physiol. (Paris) *81*, 228–236.
37. Artola, A., Bröcher, S., and Singer, W. (1990). Different voltage-dependent thresholds for inducing long-term depression and long-term potentiation in slices of rat visual cortex. Nature *347*, 69–72.
38. Sjöström, P.J., Turrigiano, G.G., and Nelson, S.B. (2001). Rate, timing, and cooperativity jointly determine cortical synaptic plasticity. Neuron *32*, 1149–1164.
39. Clopath, C., Büsing, L., Vasilaki, E., and Gerstner, W. (2010). Connectivity reflects coding: a model of voltage-based STDP with homeostasis. Nat. Neurosci. *13*, 344–352.
40. Bliss, T.V., and Lomo, T. (1973). Long-lasting potentiation of synaptic transmission in the dentate area of the anaesthetized rabbit following stimulation of the perforant path. J. Physiol. *232*, 331–356.
41. Kauer, J.A., Malenka, R.C., and Nicoll, R.A. (1988). NMDA application potentiates synaptic transmission in the hippocampus. Nature *334*, 250–252.
42. Kuba, K., and Kumamoto, E. (1990). Long-term potentiations in vertebrate synapses: a variety of cascades with common subprocesses. Prog. Neurobiol. *34*, 197–269.
43. Hanse, E., and Gustafsson, B. (1994). Onset and stabilization of NMDA receptor-dependent hippocampal long-term potentiation. Neurosci. Res. *20*, 15–25.
44. Frémaux, N., and Gerstner, W. (2016). Neuromodulated Spike-Timing-Dependent Plasticity, and Theory of Three-Factor Learning Rules. Front. Neural Circuits *9*, 85.
45. He, K., Huertas, M., Hong, S.Z., Tie, X., Hell, J.W., Shouval, H., and Kirkwood, A. (2015). Distinct eligibility traces for LTP and LTD in cortical synapses. Neuron *88*, 528–538.
46. Pfeiffer, M., Nessler, B., Douglas, R.J., and Maass, W. (2010). Reward-modulated Hebbian learning of decision making. Neural Comput. *22*, 1399–1444.
47. Seol, G.H., Ziburkus, J., Huang, S., Song, L., Kim, I.T., Takamiya, K., Huganir, R.L., Lee, H.K., and Kirkwood, A. (2007). Neuromodulators control the polarity of spike-timing-dependent synaptic plasticity. Neuron *55*, 919–929.
48. He, K., Huertas, M., Hong, S.Z., Tie, X., Hell, J.W., Shouval, H., and Kirkwood, A. (2015). Distinct Eligibility Traces for LTP and LTD in Cortical Synapses. Neuron *88*, 528–538.
49. Abe, M., Schambra, H., Wassermann, E.M., Luckenbaugh, D., Schweighofer, N., and Cohen, L.G. (2011). Reward improves long-term retention of a motor memory through induction of offline memory gains. Curr. Biol. *21*, 557–562.
50. Klein-Flügge, M.C., and Bestmann, S. (2012). Time-dependent changes in human corticospinal excitability reveal value-based competition for action during decision processing. J. Neurosci. *32*, 8373–8382.
51. Thabit, M.N., Nakatsuka, M., Koganemaru, S., Fawi, G., Fukuyama, H., and Mima, T. (2011). Momentary reward induce changes in excitability of primary motor cortex. Clin Neurophysiol *122*, 1764–1770.
52. Engelhard, B., Ozeri, N., Israel, Z., Bergman, H., and Vaadia, E. (2013). Inducing γ oscillations and precise spike synchrony by operant conditioning via brain-machine interface. Neuron *77*, 361–375.
53. Fetz, E.E. (2013). Volitional control of cortical oscillations and synchrony. Neuron *77*, 216–218.
54. Siegel, M., Donner, T.H., and Engel, A.K. (2012). Spectral fingerprints of large-scale neuronal interactions. Nat. Rev. Neurosci. *13*, 121–134.
55. Salinas, E., and Sejnowski, T.J. (2001). Correlated neuronal activity and the flow of neural information. Nat. Rev. Neurosci. *2*, 539–550.
56. Stetson, C., and Andersen, R.A. (2014). The parietal reach region selectively anti-synchronizes with dorsal premotor cortex during planning. J. Neurosci. *34*, 11948–11958.
57. Fetz, E.E., Chen, D., Murthy, V.N., and Matsumura, M. (2000). Synaptic interactions mediating synchrony and oscillations in primate sensorimotor cortex. J. Physiol. Paris *94*, 323–331.
58. Edwardson, M.A., Lucas, T.H., Carey, J.R., and Fetz, E.E. (2013). New modalities of brain stimulation for stroke rehabilitation. Exp. Brain Res. *224*, 335–358.
59. Levy, R.M., Harvey, R.L., Kissela, B.M., Winstein, C.J., Lutsep, H.L., Parrish, T.B., Cramer, S.C., and Venkatesan, L. (2016). Epidural Electrical Stimulation for Stroke Rehabilitation: Results of the Prospective, Multicenter, Randomized, Single-Blinded Everest Trial. Neurorehabil. Neural Repair *30*, 107–119.
60. McAllister, C.J., Rönnqvist, K.C., Stanford, I.M., Woodhall, G.L., Furlong, P.L., and Hall, S.D. (2013). Oscillatory beta activity mediates neuroplastic effects of motor cortex stimulation in humans. J. Neurosci. *33*, 7919–7927.
61. Plow, E.B., Carey, J.R., Nudo, R.J., and Pascual-Leone, A. (2009). Invasive cortical stimulation to promote recovery of function after stroke: a critical appraisal. Stroke *40*, 1926–1931.
62. Birbaumer, N., Ramos Murguialday, A., Weber, C., and Montoya, P. (2009). Neurofeedback and brain-computer interface clinical applications. Int. Rev. Neurobiol. *86*, 107–117.

63. Colliaux, D., Molter, C., and Yamaguchi, Y. (2009). Working memory dynamics and spontaneous activity in a flip-flop oscillations network model with a Milnor attractor. Cogn Neurodyn *3*, 141–151.

64. Izhikevich, E.M., Desai, N.S., Walcott, E.C., and Hoppensteadt, F.C. (2003). Bursts as a unit of neural information: selective communication via resonance. Trends Neurosci. *26*, 161–167.

65. Tiesinga, P.H., Fellous, J.M., Salinas, E., José, J.V., and Sejnowski, T.J. (2004). Inhibitory synchrony as a mechanism for attentional gain modulation. J. Physiol. Paris *98*, 296–314.

66. Zaepffel, M., Trachel, R., Kilavik, B.E., and Brochier, T. (2013). Modulations of EEG beta power during planning and execution of grasping movements. PLoS ONE *8*, e60060.

67. Haegens, S., Nácher, V., Hernández, A., Luna, R., Jensen, O., and Romo, R. (2011). Beta oscillations in the monkey sensorimotor network reflect somatosensory decision making. Proc. Natl. Acad. Sci. USA *108*, 10708–10713.

68. Saalmann, Y.B., Pigarev, I.N., and Vidyasagar, T.R. (2007). Neural mechanisms of visual attention: how top-down feedback highlights relevant locations. Science *316*, 1612–1615.

69. Klimesch, W., Freunberger, R., Sauseng, P., and Gruber, W. (2008). A short review of slow phase synchronization and memory: evidence for control processes in different memory systems? Brain Res. *1235*, 31–44.

70. Fahle, M. (2009). Perceptual learning and sensomotor flexibility: cortical plasticity under attentional control? Philos. Trans. R. Soc. Lond. B Biol. Sci. *364*, 313–319.

71. Little, S., Pogosyan, A., Neal, S., Zavala, B., Zrinzo, L., Hariz, M., Foltynie, T., Limousin, P., Ashkan, K., FitzGerald, J., et al. (2013). Adaptive deep brain stimulation in advanced Parkinson disease. Ann. Neurol. *74*, 449–457.

72. Rosin, B., Slovik, M., Mitelman, R., Rivlin-Etzion, M., Haber, S.N., Israel, Z., Vaadia, E., and Bergman, H. (2011). Closed-loop deep brain stimulation is superior in ameliorating parkinsonism. Neuron *72*, 370–384.

73. Cagnan, H., Pedrosa, D., Little, S., Pogosyan, A., Cheeran, B., Aziz, T., Green, A., Fitzgerald, J., Foltynie, T., Limousin, P., et al. (2017). Stimulating at the right time: phase-specific deep brain stimulation. Brain *140*, 132–145.

74. Greenblatt, R.E., and Pflieger, M.E. (2004). Randomization-based hypothesis testing from event-related data. Brain Topogr. *16*, 225–232.

STAR★METHODS

KEY RESOURCES TABLE

REAGENT or RESOURCE	SOURCE	IDENTIFIER
Experimental Models: Organisms/Strains		
juvenile male macaque nemestrina monkeys	Washington National Primate Research Center (WaNPRC)	IDs: A09150; M06212
Software and Algorithms		
MATLAB R2016a	The Mathworks	https://www.mathworks.com

CONTACT FOR REAGENT AND RESOURCE SHARING

Further information and requests for resources and reagents should be directed to and will be fulfilled by the Lead Contact, Stavros Zanos (stavroszanos@gmail.com).

EXPERIMENTAL MODEL AND SUBJECT DETAILS

Experiments were performed with healthy juvenile male macaque nemestrina monkeys, aged between 4 and 8 years old and weighing between 7 and 12 Kg. The animals were single and pair housed and during the experimental days were kept food restricted for operant conditioning. None previous procedures involved the animals used in this study. The experiments were approved by the Institutional Animal Care and Use Committee (IACUC) at the University of Washington and all procedures conformed to the National Institutes of Health Guide for the Care and Use of Laboratory Animals.

METHOD DETAILS

Intracellular recordings

Intracellular recordings were obtained in awake and anesthetized animals with glass microelectrodes advanced through a small craniotomy. The monkey was seated in the primate chair, and its head was attached to a stereotaxic frame via the implanted tubes. The stereotaxic frame provided support and repeatable reference coordinates for the electrode carriers. A small elliptical hole (2 X 3 mm) was drilled through the acrylic and the skull at a site within the region bounded by A5–A20 and L3–L20, an area that covers the anterior portion of the central gyrus. The dura was incised with a fine needle (26 gauge hypodermic) to expose the surface of the cortex. Under binocular vision electrodes for IC and EC recording were inserted into the cortex with independently movable stereotaxic carriers (Narishige SM-15 and David Kopf). The EC electrode was inserted in a vertical stereotaxic direction, and the IC electrode was inserted at an angle of 10 –20° from vertical in the parasagittal plane. The IC electrode was advanced by a pulse-stepping microdrive (Narishige, MO-71, or Burleigh Inchworm). After electrode tips were placed in the superficial cortical layer, the hole in the skull was filled with 4% agar dissolved in saline to dampen cortical pulsations. To record in waking state, the halothane was turned off and the monkey allowed to recover from the anesthesia for at least 30 min. When the monkey began performing the task, the pipettes were advanced to record IC and EC neuronal activity simultaneously. IC recordings were obtained with glass micropipettes (2 mm outer diameter) filled with 3 M KCl or K-methylsulfate with resistance between 10 and 40 MΩ. The EC electrode was a single- or multi-barreled glass micropipette. The single pipettes were broken at the tip to 2 mm and filled with 0.5 M Na-glutamate for both recording and iontophoresis. In most of the experiments, more stable recordings of isolated EC unit activity were obtained with double-barreled pipettes containing a carbon fiber of 7 mm diameter (Toray, Toreca-3000) in one barrel. The carbon fiber was exposed for 5–50 mm at the tip of the pipette, and electric signals were led to an amplifier via KCl medium. The other barrel was filled with Na-glutamate (10 mM) to activate the isolated single unit(s) iontophoretically. The carbon fiber barrel was connected to an AC amplifier, and the glutamate side was connected to a constant-current isolation amplifier for application of iontophoretic anodal current of up to 70 nA (Dia Medical, DPI-30, or Axon Instruments Axoprobe). A small platinum-plated pin implanted near the recording site was used as a reference electrode. The signals from the IC electrode were amplified to provide both low-gain DC records (0 – 10 kHz) and high-gain AC records (1 Hz to 10 kHz). All signals were recorded at 0 – 5 kHz bandwidth on an 8- or 14-channel FM tape recorder (TEAC R-30 or Honeywell 101). The local field potential was then bandpass-filtered at 25-45 Hz and a dual time-amplitude window discriminator detected cycles of oscillatory activity. A logic circuit was custom designed to deliver test stimuli at regular intervals of 1 or 2/sec and to transition to cycle-triggered stimulation when oscillatory episodes were detected. Extracellular electrodes were used to record simultaneous activity of neighboring units and field potentials, as well as to deliver microstimuli (Figure 1A). Full details of experimental procedures are described elsewhere [7, 29].

Subjects and behavioral task

During daily experimental sessions each monkey sat in a primate chair, in front of a computer screen, with both its forearms comfortably resting at the sides and flexed at the elbows. Both arms were restrained and a 3-axes accelerometer (MMA7341L, Pololu Robotics and Electronics) was taped to the back of each hand. A cursor, one for each hand, represented the root mean squared output of each accelerometer. The monkey was rewarded with fruit sauce for keeping both cursors inside a ''rest box,'' at the bottom of the screen, by not moving either hand for at least 10-15 s.

Surgical procedures and implant

During sterile surgery each monkey was anesthetized with sevoflurane gas. A midline scalp incision was made and the scalp was resected. The epidural electrodes were implanted through individual 0.5mm burr holes drilled with a stereotaxically controlled drill. The electrodes in both monkeys were located over the primary motor cortex (M1). Monkey 1 had additional electrodes over the supplementary motor cortex [31]. Monkey 1 received a total of 9 M1 electrodes and 3 SMA electrodes on each hemisphere. Monkey 2 received a total of 9 M1 electrodes on the left hemisphere. Skull screws placed remotely from the implanted areas served as tissue grounds.

The epidural electrodes were made with 9mm cut length of platinum rod (AM Systems #711000, 0.254 mm diameter) insulated with heat-shrink Pebax (Small Parts #B0013HMWJQ). Pebax was cut so that the exposed tip was ~0.5 mm. Correspondingly, the surface area of the exposed electrode tip was ~0.06 mm^2. Impedances ranged between 10 and 20 KOhms (at 1000 Hz).

Recordings

Signals from all cortical electrodes were recorded single-ended (relative to tissue ground) using two 16-channel ZC-16 headstages (Tucker-Davis, Alachua, FL) or two 16-channel, DC-coupled g.USB amplifiers (g.tec Medical Engineering Gmbh, Schiedlberg, Austria). Signals were sampled at 24-bit resolution, at 4.8 Ksamples/sec, with no filtering. Data from the amplifiers were streamed to a personal computer through a USB link, then stored and visualized in real-time using a Simulink-based (MathWorks, Natick, MA) graphical user interface, developed in-house. A trigger signal, sampled simultaneously on each of the amplifier units, was used to align recordings for analysis.

Electrical stimulation

Electrical stimuli were delivered to a pair of immediately-neighboring cortical electrodes (bipolar stimulation) by a biphasic stimulus isolator (BSI-1, BAK Electronics, Stanford, FL), driven by a pulse generator (Master-8, A.M.P.I., Jerusalem, Israel). The pulse generator was triggered by the computer running Simulink-based custom-made software. Each stimulus was a biphasic, symmetric pulse, of 0.2ms pulse width.

Closed-loop stimulation

The closed-loop system comprised an amplifier, a personal computer (PC) and the stimulator. ECoG signals were recorded by the amplifier and collected by and stored on a PC. The PC simultaneously ran custom-made Simulink software that implemented a real-time display, a band-pass (BP) filter and a dual time-amplitude window discriminator. By selecting the ECoG channel and the corner frequencies of the BP filter (beta range, 12-25 Hz), and setting the threshold (typically at 3 times the standard deviation of the beta-filtered signal from the triggering site, for the first few minutes of the recording) and the timing and amplitude parameters for the discriminator, we programmed the PC to generate triggers on specific phases of ongoing ECoG oscillations of a specific frequency, on a given channel. Those triggers were used in real-time to trigger the delivery of single-pulse, conditioning stimuli to the stimulated site. When no oscillatory episodes occurred, single test stimuli, of the same amplitude, and shape as the conditioning stimuli, were delivered at a constant rate of 2/s. The timing of all conditioning and test stimuli was recorded; the exact sequence of those stimuli was subsequently repeated during an open-loop control stimulation session.

Experimental timeline

Before any conditioning experiment was performed, cortical connectivity maps were generated, by identifying cortical sites showing CEPs when another site was stimulated. For the closed-loop experiments a given stimulated site and the triggering site were selected randomly from those sites on which CEPs had been consistently evoked during the ''mapping'' procedure. Oscillatory activity at the triggering site was used to trigger the delivery of single-pulse stimulation at the stimulated site; in the absence of oscillatory activity, test stimuli were delivered. Each of the test stimuli elicited CEPs at several recording sites, including the triggering site. Since the amplitude of those CEPs reflects the effective connectivity between the stimulated and the recording sites with CEPs, we were able to simultaneously perform the conditioning and test its effects on a spatially distributed set of sites.

Each conditioning stimulation session comprised 3 stages: (1) continuous test stimuli, 2 Hz rate, for 5 min (approximately 600 stimuli in total), (2) activity-dependent conditioning (cycle-triggered and test stimuli), for 30-40 min, (3) continuous test stimuli, 2 Hz rate, for 5 min. ECoG activity at all cortical sites, except the site that was being stimulated, was recorded simultaneously. For most of the conditioning sessions, control stimulation sessions were performed on separate days. When a control session was performed on the same day as the corresponding conditioning session, a 30 minute ''washout'' period was interposed after the conditioning and before the control session. Control stimulation consisted of the same sequence of conditioning and test stimuli delivered during the respective conditioning session, but independently of ongoing oscillatory activity. In controls for the effect of oscillatory episodes alone, the cycle-triggered stimuli were omitted and just test stimuli delivered.

Estimation of phase shift introduced by the BCI

The real-time operation of the recurrent BCI introduces time delays and phase shifts between recorded signals and generation of triggers. Time delays are introduced by the digital components (amplifiers, USB link, and computer) and the software programs running on the PC and are frequency-independent. The phase shift is introduced by the causal filtering performed in real-time by the software and can be frequency-dependent. These delays, if not accounted for, would lead to erroneous estimation of the instantaneous phase of the ECoG oscillation which triggered a stimulus.

To estimate these delays, we used a function generator to create a continuous sinusoidal signal, with a constant frequency (from 12 to 25 Hz, in 1- or 2-Hz steps). The signal was input to one of the channels of a digital oscilloscope. The same signal was also fed into the chain of components comprising the closed-loop BCI system: headstage, amplifier, computer, software, trigger line, stimulator. We used the GUI to trigger the stimulator from an arbitrarily-selected phase of the sinusoidal oscillation. The output monitor of the stimulator was fed into a second input channel of the digital oscilloscope and registered. The phase of the original oscillation at which the stimulation trigger was registered on the oscilloscope was then compared with the oscillatory phase from which stimulation was triggered at the GUI. These phases were estimated by the method described below ("Estimation of stimulation phase"). The difference between the 2 phases, $\Delta\varphi$, was finally converted to a temporal delay introduced by the closed-loop system, Δt, for signal frequency f:

$$\Delta t = \frac{1}{f}\frac{\Delta\varphi}{2\pi}$$

QUANTIFICATION AND STATISTICAL ANALYSIS

Cortically-evoked potentials

Stimulus-triggered averages of ECoG activity on all recording sites were compiled to identify cortically-evoked potentials (CEPs) and those CEPs were then used to assess the effects of conditioning on effective connectivity. To assess the effect of bursts of conditioning stimuli, cortical responses to test stimuli delivered immediately before bursts were compared to responses to test stimuli delivered immediately after bursts. Bursts of 2, 3, 4 or 5 successive stimuli, i.e., with inter-stimulus intervals less than 75 ms, were studied separately. To assess the decay of conditioned effects, we registered cortical responses to test stimuli delivered 0.5, 1, 1.5 and 2 s after the conditioning burst. To assess the longer-term effect of conditioning, CEPs to about 500 test stimuli delivered consecutively before the conditioning started were compared to CEPs to 500 test stimuli delivered after the end of conditioning.

In all CEPs shown in this paper, stimulation artifacts were removed on a single-sweep basis by blanking out the artifact samples (typically 1-1.5ms post-stimulus).

To assess whether there was a significant difference in the CEPs associated with two different sets of test stimuli (e.g., test stimuli immediately before and immediately after a conditioning burst) we used a randomization-based, non-parametric method for making within-subject, between-conditions, event-related potential comparisons [74]. In this test, the actual differences in the voltage means, across sweeps, at each sample between the two conditions are compared to the 99th percentile of the distribution of 1000 surrogate differences between pairs of means. Each of these surrogate differences is generated by shuffling the labels of all sweeps registered in both conditions, and randomly assigning the sweeps to one of two surrogate conditions; the difference between the means associated with these two surrogate conditions constitutes one of the 1000 surrogate differences. The test returns the indices of the samples in the stimulus-triggered averages that are statistically significantly different, at the 0.001 confidence level, between the two conditions. For such differences to be considered physiologically meaningful we required that there was at least a 3 ms-long epoch of contiguous samples that were significantly different between the two conditions, occurring 3 to 10 ms post-stimulus. This criterion ensured that variability scattered throughout the duration of the CEPs was not deemed a significant difference.

The amplitude of a CEP was defined as the maximum, positive or negative, deflection from baseline (average of samples between 5 and 30 ms pre-stimulus) between 3 and 8 ms post-stimulus, i.e., the amplitude of the first phase of the CEP. That peak deflection had to exceed 2 standard deviations of the baseline signal, otherwise it was assumed that there was no CEP on that site. The latency at which CEP amplitude was measured was determined through several additional criteria. First, a positive (or negative) peak had to occur within a segment at least 2-ms long of contiguous positive (or negative) voltage samples; this criterion ensured that very fast and brief stimulus artifacts were not regarded as CEPs. Second, the second derivative of the CEP around the peak should be close to zero. Third, the difference between the sample with the maximum deflection and its neighboring two samples (before and after) could not exceed 5% of the maximum deflection value. These two last criteria ensured that the shape of the CEP around its peak was not corrupted by an electrical or other artifact. The CEP amplitude was then calculated as the average of those 3 samples.

Estimation of stimulation phase

The instantaneous oscillatory phase of the ECoG signal at the triggering or a non-triggering recording site at the time a stimulus was delivered (instantaneous stimulation phase, ISP) was estimated by fitting a sinusoidal signal Y of unknown amplitude A, unknown period T and unknown initial phase φ_0 to a DC-corrected stimulus-triggered ECoG sweep extending from about 60 ms before the stimulus to the stimulus time, according to the following equation:

$$Y(t) = A * \sin\left(\varphi_0 + 2\pi\frac{t}{T}\right)$$

A nonlinear least-squares fitting method was used for the fitting, using the Levenberg-Maquardt algorithm, implemented with MATLAB's Curve Fitting toolbox. Goodness of fit of a sinusoid to a single ECoG sweep, or to a stimulus-triggered average (Figure 5), was assessed by calculating the coefficient of determination (R^2).

Instantaneous phase φ at t_{STIM} (i.e., at the time of stimulation) was then calculated by:

$$\varphi = \varphi_0 + 2\pi \frac{t_{STIM}}{T}$$

Fitting the raw ECoG signal or the filtered ECoG signal (between 12-25 Hz) did not generate different instantaneous stimulation phase estimates, or goodness of fit. Limiting instantaneous phase estimation to sweeps that were fitted the best (e.g., with an R^2 value of more than 0.8) did not change the average and standard deviation of the estimated phase distribution.

DATA AND SOFTWARE AVAILABILITY

Data and code available upon request to the Lead Contact, Stavros Zanos (stavroszanos@gmail.com).